Journal of Magnetic Resonance 210 (2011) 82–89

Contents lists available at ScienceDirect

Journal of Magnetic Resonance

journal homepage: www.elsevier.com/locate/jmr

Geometry of kinked protein helices from NMR data

Dylan T. Murray [a], Yuanting Lu [b], T.A. Cross [a], J.R. Quine [b,*]

[a] Institute of Molecular Biophysics, Florida State University, Kasha Laboratory, Tallahassee, FL 32306, United States
[b] Department of Mathematics, Florida State University, 208 Love Building, 1017 Academic Way, Tallahassee, FL 32306, United States

ARTICLE INFO

Article history:
Received 16 December 2010
Revised 6 February 2011
Available online 16 February 2011

Keywords:
Alpha helix
Frenet frame
Quaternion
Ramachandran diagram
SSNMR
Membrane protein
Protein structure
PISEMA
PISA wheel
Orientational restraints
Torsion angle
Chemical shift
Dipolar coupling
Eyrings formula

2000 Mathematical Subject Classification:
Primary 92E10
Secondary 51P99

ABSTRACT

Mathematical questions related to determining the structure of a protein from NMR orientational restraints are discussed. The protein segment is a kinked alpha helix modeled as a regular alpha helix in which two adjacent torsion angles have been varied from their ideal values. Varying these torsion angles breaks the helix into two regular helical segments joined at a kink. The problem is to find the torsion angles at the kink from the relationship of the helical segments to the direction of the magnetic field.

1. Introduction

1.1. Membrane proteins

Fine structural detail is important for understanding the functional mechanisms of membrane proteins. For channels conducting ions the mechanism requires a precise alignment of the atoms near the active site. In the M2 protein from influenza A, for example, it is known [1] that a glycine is one of the most conserved amino acids in the evolution of the protein. A detailed knowledge of the structure near that residue will help in understanding why it is conserved, and why it is important in conduction of protons [2]. One possibility is that the helix forms a kink there. Either the kink at Gly helps to align the other residues in the helix properly, or else the kink exposes a carbonyl oxygen to function in conduction of the ions. This paper explores a model in which NMR orientation restraints can provide information on the structure at a kink.

1.2. NMR orientational restraints

Orientational restraints are obtained from NMR spectra of samples that are uniformly aligned with respect to the magnetic field. These orientational restraints are obtained from a class of separated local field experiments that represents refinements [3,4] on the PISEMA experiment [5]. Utilizing these restraints has been described in detail [6–8] [9]. If proteins are put in a fixed orientation in a magnetic field, the signal from the nuclear spins in the molecule is dependent on the orientation of the sample, and one can find the coordinates of the unit magnetic field direction in molecular frames rigidly attached to the molecule. This approach has been used to characterize the structure of quite a few membrane protein structures [10,1,11–20].

Orientation dependent structural restraints can also be obtained in solution NMR experiments through residual dipolar coupling (RDC) measurements of proteins in partially oriented

* Corresponding author.
E-mail addresses: dmurray@magnet.fsu.edu (D.T. Murray), cross@magnet.fsu.edu (T.A. Cross), quine@fsu.edu (J.R. Quine).

1090-7807/$ - see front matter © 2011 Elsevier Inc. All rights reserved.
doi:10.1016/j.jmr.2011.02.012

media. The incorporation of RDC measurements has allowed structural characterization of large soluble proteins [22,23] as well as large membrane proteins [24]. RDC values obtained from membrane proteins solubilized in detergent micelles provide an opportunity to characterize protein secondary structure topology. Secondary structure dependent patterns are expected for RDC spectra [25] which allows the direct comparison of secondary structure topologies determined from both solution and solid state NMR. These techniques are becoming common for membrane proteins [26–29,14].

1.3. Kinked alpha helix

In NMR experiments such as PISEMA an alpha helix shows a resonance pattern called a PISA wheel, and the angle between the helix axis and the magnetic field direction can be found from the pattern [32,9,8,16]. This angle is called the *tilt angle* and is denoted τ. When this helix is a segment of a membrane protein in a lipid bilayer, and the bilayer normal is parallel to the magnetic field direction, τ also gives the tilt of the helix in the membrane. When PISEMA shows two distinct resonance patterns for a single helix, this indicates a kinked alpha helix with two straight alpha helical segments, and the tilt angles τ and τ' for each segment can be found.

Of more importance in understanding the protein structure is the *kink angle* κ, the angle between axes of the two helical segments. This cannot be determined from τ and τ' alone. From elementary considerations, κ is between $|\tau'-\tau|$ and $\tau' + \tau$ (For proteins crossing the membrane, the tilt angle can be assumed to be between 0° and 90°.).

To find the kink angle, more information than the two tilt angles is needed (see Fig. 1). For each alpha helical segment, the PISEMA experiment is capable of finding a rotation angle ρ in addition to the tilt angle τ. The angles ρ, τ are the spherical coordinates of the magnetic field direction in a frame rigidly attached to the straight alpha helix segment. This frame is referred to as a *helix axis frame*.

Given a simplified model of a kinked alpha helix, the kink angle κ can be found from the angles ρ, τ and ρ', τ'. This paper explains the model and the method of solving for the kink angle. In the model, a kinked alpha helix is a pair of straight alpha helix segments with uniform ϕ_0, ψ_0 torsion angles except for two torsion angles varied from ϕ_0, ψ_0 at a single alpha carbon between them where the kink is formed. Now the angles ϕ, ψ can be solved given ρ, τ and ρ', τ', and from ϕ, ψ the kink angle κ can be computed. The calculation is carried out in a very general fashion so that the solution is in terms of ϕ_0, ψ_0 and the various bond angles along the backbone, and these can be chosen appropriate to the protein environment.

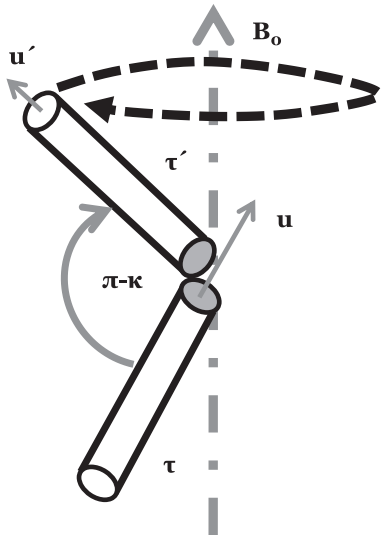

Fig. 1. A kinked helix with segments having tilt angles τ and τ'. B_0 is the unit direction of the magnetic field and also the normal to the membrane bilayer surface. The nitrogen atoms of the straight helical segments lie on the two cylinders. Rotating helix 2 about B_0 does not change the tilts and gives values of the kink angle κ in the range $|\tau' - \tau| \leqslant \kappa \leqslant \tau' + \tau$. The kink angle cannot be found from the two tilt angles alone.

1.4. Mathematical tools

A string of bonded atoms such as the backbone of a protein can be thought of as a sequence of points in space, a discrete curve. Finding the shape of this curve is one important step in determining structure. In the differential geometry of smooth curves the Frenet frame is used to describe the shape of the curve in terms of curvature and torsion. A modification of the Frenet frame is used here to explicitly write the transformation between frames in terms of torsion angles and bond angles. The transformations can be written using rotation matrices or quaternions. Similar computations are found in earlier papers [30,31]. The concept of a Frenet Frame unifies these ideas in terms of differential geometry of discrete curves.

Given a frame at a nitrogen on the helix, the frame at the subsequent nitrogen is given by rotating this frame about the helix axis. (Since we are concerned only with orientations, the translation is ignored.) For an alpha helix the rotation angle is approximately 100°, giving 3.6 nitrogen atoms on the backbone per turn of the helix. This rotation angle and axis can be computed in terms of torsion angles and bond angles using Frenet frame calculations.

A regular alpha helix is one whose torsion angles are the same at each alpha carbon. The torsion angles are fixed at ideal values denoted ϕ_0 and ψ_0 in the region of the Ramachandran plane for alpha helices. A kinked helix is formed by taking a single regular alpha helix and varying from the ideal values two torsion angles ϕ and ψ at an alpha carbon near the middle of the helix. These torsion angles parameterize the kink. The resulting kinked helix is formed by two regular alpha helical segments. The angle between the axes of the helical segments is called the kink angle κ.

The orientation of the segments is given by frames H_1 and H_2 for the first and second segments respectively. The third vector in the frame H_1 is in the direction of the axis of the first helical segment and similarly for H_2. For this reason they are referred to as helix axis frames. The frames are chosen to be fixed in one of the molecular frames along the helix segment. The orientation of the helix segments with respect to the unit magnetic field B_0 can be found if the coordinates of B_0 in each of the two frames is known. If the coordinates of B_0 in the frames H_1 and H_2 are given by vectors X_1 and X_2 respectively, then $H_1X_1 = H_2X_2$. This gives an equation of the form $X_2 = H_2^* H_1 X_1$, and since X_1 and X_2 are unit vectors, this vector equation gives essentially two equations for ϕ and ψ. If X_1 and X_2 are found from the experiment (usually in terms of spherical coordinates ρ, τ and ρ', τ', the equations can be solved for the torsion angles ϕ and ψ at the kink, giving the structure of the kinked helix. The kink angle κ can then be computed in terms of the torsion angles ϕ and ψ, Eq. (15).

2. Frenet frames

Here we discuss the Frenet frames for a discrete curve. If $\mathbf{p}_j$ is a sequence of points in 3D space then unit tangent vectors are defined by

$$\mathbf{t}_j = \frac{\mathbf{p}_{j+1} - \mathbf{p}_j}{|\mathbf{p}_{j+1} - \mathbf{p}_j|},$$

and if adjacent tangent vectors are not parallel, binormal vectors by

$$\mathbf{b}_j = \frac{\mathbf{t}_{j-1} \times \mathbf{t}_j}{|\mathbf{t}_{j-1} \times \mathbf{t}_j|}$$

and normal vectors by

$$\mathbf{n}_j = \mathbf{b}_j \times \mathbf{t}_j.$$

The Frenet frames are

$$F_j = (\mathbf{t}_j, \mathbf{n}_j, \mathbf{b}_j), \tag{1}$$

which may be thought of as a 3×3 matrices with column vectors $\mathbf{t}_j$, $\mathbf{n}_j$, $\mathbf{b}_j$.

Curvature angles α_j at $\mathbf{p}_j$ and torsion angles τ_j about $\mathbf{t}_j$ can be defined by

$$R(\mathbf{b}_j, \alpha_j)\mathbf{t}_{j-1} = \mathbf{t}_j$$
$$R(\mathbf{t}_j, \tau_j)\mathbf{b}_j = \mathbf{b}_{j+1}.$$

Here $R(\mathbf{u},\eta)$ indicates counterclockwise rotation an angle η about the vector u.

The rotation from one Frenet frame to the next is given by

$$R(\mathbf{b}_{j+1}, \alpha_{j+1})R(\mathbf{t}_j, \tau_j)F_j = F_{j+1} \tag{2}$$

or equivalently

$$F_j R_x(\tau_j)R_z(\alpha_{j+1}) = F_{j+1} \tag{3}$$

where R_x and R_z are rotations about the x and z axes, given by the rotation matrices

$$R_x(\eta) = \begin{pmatrix} 1 & 0 & 0 \\ 0 & \cos\eta & -\sin\eta \\ 0 & \sin\eta & \cos\eta \end{pmatrix} \quad R_z(\eta) = \begin{pmatrix} \cos\eta & -\sin\eta & 0 \\ \sin\eta & \cos\eta & 0 \\ 0 & 0 & 1 \end{pmatrix}. \tag{4}$$

Eq. (3) is essentially the same as formula (1) in [21 and is sometimes referred to as Eyring's formula.

2.1. Helix axis frame

A helix axis frame is defined at each nitrogen on the backbone of a regular helix. The third vector in the helix axis frame is the helix axis and the first two vectors are perpendicular to the axis. The helix axis frame H is chosen so that it is constant in relation to the Frenet frame, i.e., $F * H$ is the same at each nitrogen atom. (Here $*$ denotes the transpose.) Usually just one of these frames is chosen to orient the helix segment, but since for an alpha helix the frames rotate approximately 100° about the axis as we go to successive nitrogen atoms, the orientation of one frame gives the orientation of all the others.

NMR experiments can find the coordinates of the unit magnetic field direction in all helix axis frames for a regular helix. In particular, an experiment called PISEMA can find these coordinates from a resonance pattern called a PISA wheel [19,9].

The computations in Appendix A give coordinates of the helix axis in the Frenet frame at the nitrogen. An approximation made there is that the bond angles at the nitrogen and carbonyl carbon are the same and that the geometry at the alpha carbon is tetrahedral, $\cos\gamma = 1/3$. This leads to simple mathematical expressions for quantities of interest. The computations can be refined by changing these bond angles to the desired values.

To write the coordinates of the helix axis in the Frenet frame at the nitrogen, let

$$s = \frac{\phi + \psi}{2} \quad t = \frac{\phi - \psi}{2}.$$

where ϕ and ψ are parameters for the regular helix. Let

$$A = A(s) = \frac{\cos\frac{\gamma}{2}\cos s}{\sqrt{1-a^2}} = \cos s\left(\frac{2}{1+2\cos^2 s}\right)^{1/2}.$$
$$B = B(s) = \frac{\sin\frac{\gamma}{2}}{\sqrt{1-a^2}} = \left(\frac{1}{1+2\cos^2 s}\right)^{1/2}. \tag{5}$$

Now $A^2 + B^2 = 1$ and it follows from (26) that the unit helix axis is given by

$$\mathbf{u} = F\begin{pmatrix} A \\ B\cos t \\ B\sin t \end{pmatrix} = FR_x(t)\begin{pmatrix} A \\ B \\ 0 \end{pmatrix}. \tag{6}$$

where F is the Frenet frame at N.

A helix axis frame can be defined by projecting the unit tangent vector $\mathbf{t}$ perpendicular to $\mathbf{u}$ to get the first vector. The axis $\mathbf{u}$ is the third vector, and the second vector is the cross product of $\mathbf{u}$ with the first. The sequence of vectors forms a right handed orthonormal frame given by

$$H = F\begin{pmatrix} B & 0 & A \\ -A\cos t & \sin t & B\cos t \\ -A\sin t & -\cos t & B\sin t \end{pmatrix} = FR_x(t)M(s) \tag{7}$$

where $M = M(s)$ is defined by

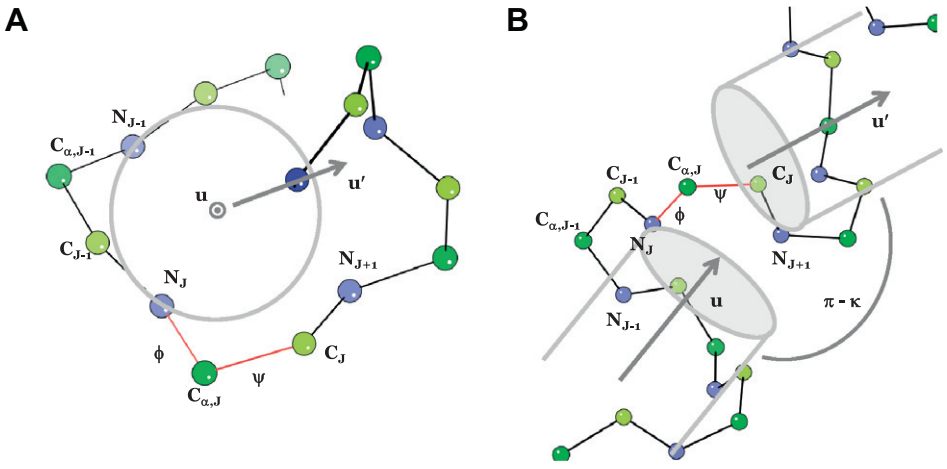

Fig. 2. A kinked alpha helix. The kink begins at the alpha carbon $C_{\alpha J}$. All the nitrogens up to N_J are on a cylinder whose axis is u. The subsequent nitrogens starting at N_{J+1} are on a cylinder whose axis is u'. The angle between the axes is κ. The torsion angles ϕ, ψ at $C_{\alpha J}$ determine κ. If these angles are equal to the standard torsion angles ϕ_0, ψ_0, then $\kappa = 0$. (A) View down the axis of the first straight helix segment. The circle in the figure is the cylinder containing the nitrogens on the first helix. (B) Side view.

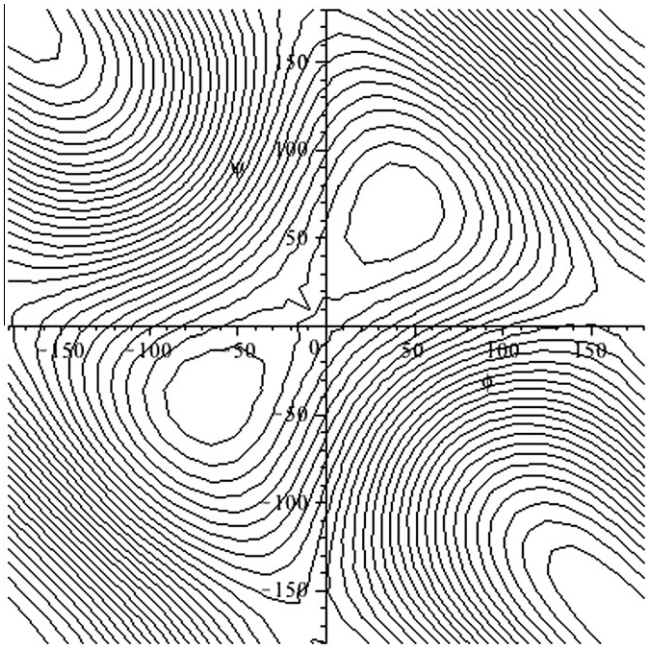

Fig. 3. Plot of level curves of $\cos\kappa$ for $\phi_0 = -65°$, $\psi_0 = -40°$. The maxima near the center are $\cos\kappa = 1$ at (ϕ_0, ψ_0) and $(-\psi_0, -\phi_0)$. The saddle point near the origin is $\cos\kappa \approx .88$ at $(t_0, -t_0)$ where $t_0 = (\phi_0; -\psi_0)/2$.

Table 1
Structure solutions for a kinked alpha helix with $\tau = 15.0°$ and $\tau' = 25.0°$. The first helical segment has fixed orientation, $\rho = 0.0°$, while the second helix segment orientation is varied by $-\Delta\rho$.

$\Delta\rho$ (°)	ϕ (°)	ψ (°)	κ (°)
0	−72.6	−52.7	11.0
	47.6	18.3	37.5
70	−102.4	−28.1	29.5
	77.4	43.7	33.0

$$M = \begin{pmatrix} B & 0 & A \\ -A & 0 & B \\ 0 & -1 & 0 \end{pmatrix}. \tag{8}$$

3. Kinked alpha helix

When a resonance pattern from PISEMA shows two PISA wheels instead of one, this may indicate a kinked helix, that is, two different regular helical segments joined together.

We define a kinked alpha helix as a backbone structure with ϕ, ψ angles equal to ideal alpha helical values ϕ_0, ψ_0 except at the kink where ϕ and ψ remain variable. See Fig. 2. We refer to the regular helix before the kink as the first helix and the regular helix after the kink as the second helix. We study the angle between the axes of the two regular helices and the change of the helix axis frame between the helices as functions of (ϕ, ψ).

3.1. Notation for kinked helix

To set up the notation let F_j be the Frenet frames and H_j the helix axis frames at the N atoms along the kinked helix. Let ϕ_0 and ψ_0 be the parameters of the regular helices and let

$$s_0 = \frac{\phi_0 + \psi_0}{2} \quad t_0 = \frac{\phi_0 - \psi_0}{2}.$$

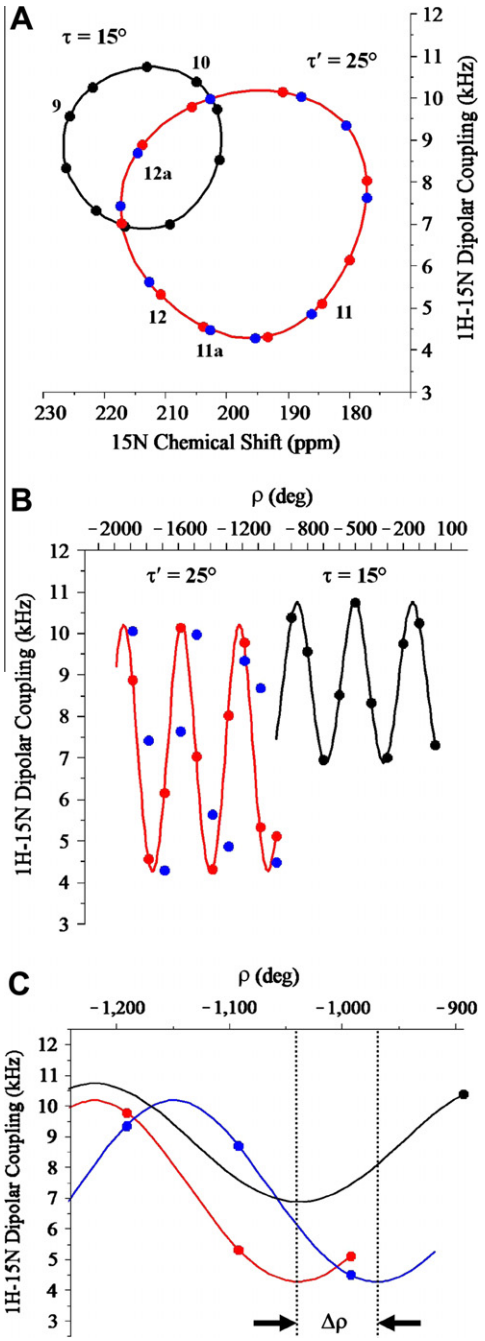

Fig. 4. Theoretical PISEMA data for a kinked alpha helix with $\tau = 15.0°$ and $\tau' = 25.0°$. Black data corresponds to the first segment of helix while the red and blue data represent two orientations of the second segment of helix that differ by $\Delta\rho = 70.0°$ (see text). The circles indicate the positions of the resonances while the curves represent the theoretical data for all values of ρ and ρ'. Numbers by the resonances indicate the residue number in the helix primary sequence and suffix a indicates the data with a nonstandard shift in ρ. (A) The PISA wheel representation of the data. (B) The dipolar wave representation of the data. (C) Close up of the site of the kink from panel B where $\Delta\rho$ can be calculated.

Define rotation matrices T and S_0 by

$$S_0 = R_x(t_0)M(s_0) \text{ and } T = T(\phi, \psi) = R_x(\phi)R_z(\gamma)R_x(\psi)R_x(\pi). \tag{9}$$

and let $T_0 = T(\phi_0, \psi_0)$. By (7), frames H_j and F_j on a regular alpha helix are related by

$$H_j = F_j S_0. \tag{10}$$

Suppose F_J is the Frenet frame before the kink, then by (29) the subsequent frame is given by

$$F_{J+1} = F_J T. \tag{11}$$

where $T = T(\phi,\psi)$ and ϕ and ψ are the torsion angle between the regular alpha helical segments. It follows that

$$H_{J+1} = H_J S_0^* T S_0.$$

If $T = T_0$ then there is no kink, the helix is a regular alpha helix, and the third vector in both frames H_J and H_{J+1} is the axis of the helix. It follows that

$$S_0^* T_0 S_0 = R_z(\theta_0). \tag{12}$$

3.2. The kink angle κ

As we saw, κ cannot be found from the tilt angles of the helix segments. It is, however, a function of the angles ϕ and ψ at the kink. In this section the angle κ between the two helix segments is found as a function ϕ and ψ.

The axis of the first helix is the third column of H_J, and the axis of the second is the third column of H_{J+1}, so $\cos\kappa$ is the 3, 3 entry of

$$H_J^* H_{J+1} = S_0^* T S_0. \tag{13}$$

By (9) this can be written as

$$\begin{aligned}\cos\kappa &= M_3(s_0)^* S_0^* T S_0 M_3(s_0)\\ &= M_3(s_0)^* R_x(\phi - t_0) R_z(\gamma) R_x(\psi + t_0) R_x(\pi) M_3(s_0).\end{aligned} \tag{14}$$

where $M_3 = (A,B,0)'$ is the third column of M. Using the tetrahedral geometry equation $\cos\gamma = \frac{1}{3}$ (14) gives the fairly simple formula

$$\begin{aligned}\cos\kappa = [3(1+2\cos^2 s_0)]^{-1}[&2\cos^2 s_0 + 4\cos s_0\cos(\varphi - t_0)\\ &+ 4\cos(\psi + t_0)\cos s_0 - \cos(\psi + t_0)\cos(\varphi - t_0) + 3\\ &\times \sin(\varphi - t_0)\sin(\psi + t_0)].\end{aligned} \tag{15}$$

Fig. 3 shows the level curves in ϕ, ψ space of $\cos\kappa$ as a function of ϕ, ψ, where $\phi_0 = -65°$ and $\psi_0 = -40°$ are set at a fixed value for an alpha helix.

Note that the right hand side of (15) is invariant under the transformations

$$(\phi - t_0, \psi + t_0) \to (\psi + t_0, \phi - t_0). \tag{16}$$

$$(\phi,\psi) \to (-\psi,-\phi) \tag{17}$$

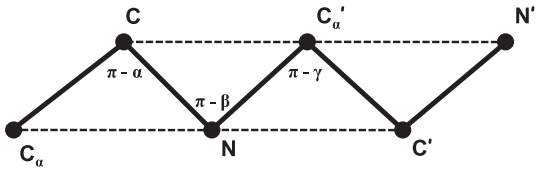

Fig. 6. Schematic drawing of protein backbone geometry. The primes indicate subsequent atoms of the same type. The planes $C_\alpha CN$ and CNC'_α are parallel. The dihedral angle from CNC'_α to $NC'_\alpha C'$ is the ϕ torsion angle and the dihedral angle from $NC'_\alpha C'$ to $C'_\alpha C'N'$ is the ψ torsion angle. The bond at the C_α is tetrahedral with γ approximately 70.5°. The angles α and β are approximately 60°.

These symmetries are seen in Fig. 3. Also note that substituting $\phi = \phi_0$ and $\psi = \psi_0$ in (15) gives $\cos\kappa = 1$, since the helix is straight and $\kappa = 0$.

4. Finding a structure

4.1. Solving for ϕ and ψ

The PISEMA experiment can determine the coordinates of the unit magnetic field direction B_0 in helix axis frames for each segment of a kinked helix. From this we show how to compute the ϕ, ψ angles at the kink.

Subsequent helix axis frames in a segment are related by $H_{j+1} = H_j R_z(\theta_0)$ where θ_0 is the rotation angle for the ideal alpha helix with parameters ϕ_0, ψ_0. The angle θ_0 can be computed from (28) and is approximately 100° for an alpha helix. If the coordinates B_0 are known in any one helix axis frame in a segment then it can be found in all the others. So assume that we have the coordinates of B_0 in frames H_J and H_{J+1} at the kink.

Spherical coordinates τ and ρ are used for B_0. Let

$$X(\rho,\tau) = \begin{pmatrix}\sin\tau\cos\rho\\ \sin\tau\sin\rho\\ \cos\tau\end{pmatrix} \tag{18}$$

be the coordinates of B_0 in the helix axis frame H_J, so that

$$B_0 = H_J X(\rho,\tau). \tag{19}$$

Similarly suppose that ρ', τ' are spherical coordinates of B_0 in the frame H_{J+1}, so that

$$B_0 = H_{J+1} X(\rho',\tau'). \tag{20}$$

The angles τ and τ' are referred to as the *tilt angles*.

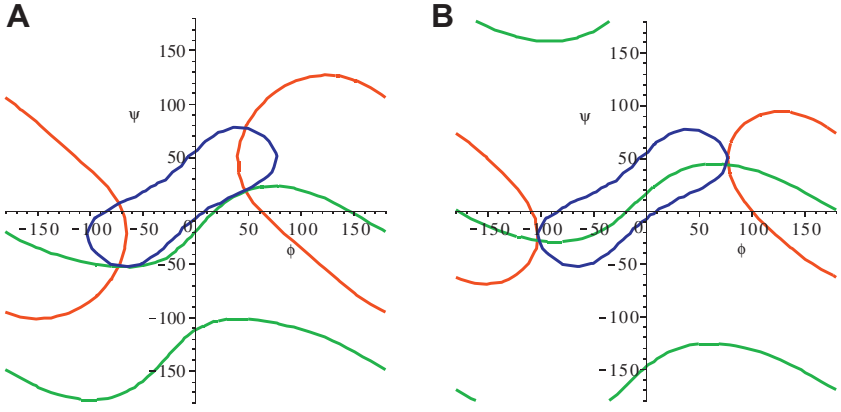

Fig. 5. Graphical representation of the solutions to the vector Eq. (21) for two different orientations of the second helical segment. The red, green and blue curves represent the first, second and third coordinates of (21) respectively. (A) Solutions for $\tau = 15.0°$, $\tau' = 25.0°$, $\rho = 0.0°$, and $\rho' = -992.5°$. (B) Solutions for $\tau = 15.0°$, $\tau' = 25.0°$, $\rho = 0.0°$, and $\rho' = -1062.5°$.

From the PISEMA experiment τ, τ', ρ, and ρ' can be found. From this the torsion angles ϕ and ψ can be found and then using (15) the kink angle κ can be found. We have

$$X(\rho',\tau') = H^*_{J+1}H_J X(\rho,\tau) = S^*_0 T(\phi,\psi)^* S_0 X(\rho,\tau) \quad (21)$$

The vector Eq. (21) gives three equations for the two variables ϕ, ψ. Since the vector X is a unit vector, the value of two coordinates gives the third up to a factor ±1. So there are essentially two equations which can be solved for ϕ and ψ. Note that if $\phi = \phi_0$ and $\psi = \psi_0$ then by (12), Eq. (21) becomes $X(\rho',\tau') = R_z(-\theta_0)X(\rho,\tau)$ and $\tau = \tau'$ and $\rho' = \rho - \theta_0$.

Finding a protein structure compatible with the data can now be done. The first and third coordinates of the Eq. (21) give two level curves in the ϕ, ψ Ramachandran plane and the intersection gives possible values of the the torsion angle at the kink. The second coordinate of Eq. (21) should be checked at each of these values.

4.2. Example structure

The utility of the calculation is best shown through an example. Suppose we have an alpha helix composed of 20 amino acids. The helix structure is kinked in the middle such that 10 residues lie on either side of the kink site. Using the notation of Section 3.1, $J = 10$. The two segments have tilt angles $\tau = 15.0°$ and $\tau' = 25.0°$. Expected ^{15}N anisotropic chemical shift and ^{1}H–^{15}N dipolar coupling experimental data can be calculated for the helical segments according to the method of Denny et al. [32], using a dipolar coupling constant of 10.735 kHz and ^{15}N anisotropic chemical shift tensor elements of $\delta_{11} = 228$, $\delta_{22} = 80$, $\delta_{33} = 57$ ppm.

Two cases are examined here. The first helical segment remains fixed with orientation angle $\rho = 0°$ as defined by the coordinates of B_0 in H_1, the helix axis frame at the first nitrogen on the helix. So as defined by (19), $\rho = -9\theta_0$. The second helix orientation angle is defined at residue 11 and is chosen to be either the expected value for a uniform alpha helix, $\rho' = -10\theta_0$, or with a larger rotation of $\rho' = -9\theta_0 - (\theta_0 + \Delta\rho)$. The angle θ_0 is given by (30) and is approximately 100° in the calculation described here. Choosing $\Delta\rho = 70.0°$ for the latter case produces the two sets of PISEMA data presented in Fig. 5A. The data for the first segment of helix remains constant for both cases (black data). Note that the change in the ρ' value has changed the position of the resonances on the PISA wheel pattern for the second segment of the helix (compare red and blue data).

The method outlined in Section 4.1 is now applied to the hypothetical experimental data for the two helix systems. The intersections of the three curves dictated by Eq. (21) give the torsion angle solutions satisfying the experimental data. The solutions are found by plotting level curves, see. The ϕ, ψ solutions are presented in Table 1 along with the corresponding kink angles. For the cases examined here only two solutions exist for each set of data, and in each set the two solutions lie in distinct regions of ϕ, ψ space.

In most cases, only torsion angles in the bottom left quadrant of ϕ, ψ space are valid structures. Based on stereochemical considerations for dipeptides the solutions lying in the left handed alpha helical region are only worth considering for cases where glycine residues are present at the kink site. Amino acids with extended side chains are predicted to have severely restricted ϕ, ψ values and in particular ϕ should not be larger than zero [33]. The other amino acids encounter steric clash between the side chain and the polypeptide backbone. However, it is worth noting that many protein structures in the PDB have torsion angles in sterically disallowed regions of ϕ, ψ space [34]. Presumably these torsion angles are permitted by steric compensation from the nearby structure in the protein, a view supported by statistical reviews of protein structures showing that the observed clustering of torsion angles in protein structures is dependent on the type of secondary structure [35] and amino acid side chain type [36]. For the cases presented here ($\Delta\rho = 0°$ and 70°) the sterically the sterically favorable torsion angle solutions for right handed alpha helical structures give kink angles for the helices of 11.0° and 29.5°. A helical model for the larger kink angle was calculated and is presented in Fig. 2.

Changes in the helix orientation of the second half of a kinked helix can represent drastically different kinked helix structures. The helix orientation can be determined precisely for uniform helices using PISEMA experiments and is easily viewed using the dipolar wave [37] analysis shown in Fig. 4B.

Deviations from the ideal PISA pattern are easily observed using chemical shift or dipolar wave analysis [20, 38, 39] which is sensitive to gradual changes in helix tilt and periodicity as well as detecting kink sites [40]. The dipolar wave analysis for the model kinked helix system is shown in Fig. 4B.

Examining the latter segment of the helix system (red and blue data) reveals that the resonances for the second set of data have distinctly different phase than the first set of data indicating that a non-uniform (i.e. not 100°) change in ρ has occurred. The change in phase, $\Delta\rho$, is the deviation of the observed resonances from the values expected if the second helix had the same phase as the first segment of helix. Calculation of $\Delta\rho$ can be seen in Fig. 4C. For any set of fixed tilt angles the phase change is linked directly to the structure of the helix kink through a three step process: (1) fit the PISEMA data giving helix tilt and rotation parameters for both helix segments, (2) use the parameters in the gram matrix equation to get the possible ϕ, ψ solutions and (3) use the ϕ, ψ solutions Eq. (15) to get the kink angle.

In conclusion, when two distinct PISA wheel patterns are observed for a single helix and helix orientations can be determined for each segment then the structure of the kink can be calculated under the assumption that the structure of the helix is approximated by a single set of non-ideal torsion angles joining two ideal helical segments.

4.3. List of variables

Symbol	Meaning	Reference
α, β, γ	acute bond angle at C, N, C_α resp.	Fig. 6
κ	angle between axes of helixes 1 and 2	Eqs. (13) and (14)
$\Delta\rho$	$\rho - \rho' - \theta_0$	Section 4.2
ϕ, ψ	torsion angles at C_α	
ϕ_0, ψ_0	standard torsion angles for alpha helix	
ρ, τ	rotation and tilt angle for helix 1	Eq. (19)
ρ', τ'	rotation and tilt angle for helix 2	Eq. (20)
θ_0	rotation angle about the helix axis to subsequent residue for regular helix with standard torsion angles ϕ_0, ψ_0.	Eq. (29)
s, t	$(\phi + \psi)/2$, $(\phi - \psi)/2$	
s_0, t_0	$(\phi_0 + \psi_0)/2$, $(\phi_0 - \psi_0)/2$	
B_0	unit direction of magnetic field	
F_j	jth Frenet frame	Eq. (1)
H_j	jth helix axis frame	Eq. (7)
S_0	rotation from F to H for regular helix with standard torsion angles ϕ_0, ψ_0.	Eq. (10)
$T(\phi,\psi)$	rotation to next Frenet frame at N	Eq. (11)
$X(\rho,\tau)$	rectangular coords as function of spherical coords	Eq. (18)

Appendix A

A.1. Rotations

Computation using Frenet frames is done by multiplying a sequence of rotations. These can be written in terms of the matrices R_x and R_z, but it is sometimes convenient to use quaternions. The rotation $R(\mathbf{u},\theta)$ can be written in terms of the unit quaternion

$$q = e^{\mathbf{u}}\frac{\theta}{2} = \cos(\theta/2) + \sin(\theta/2)\mathbf{u}$$

where the vector $\mathbf{u} = (u_1,u_2,u_3)$ is identified with the quaternion $\mathbf{u} = u_1I + u_2J + u_3K$. The action of q on any vector X is given by $X \to qXq^*$ where $q^* = \cos(\theta/2) - \sin(\theta/2)u$ is the conjugate quaternion. The result is the same as $R(\mathbf{u},\theta)X$. Multiplication of rotations can be done by multiplying the corresponding quaternions using the rules

$$I^2 = J^2 = K^2 = IJK = -1.$$

The advantage of using quaternions is that the axis of the resulting rotation can be found as the vector part of the quaternion. The scalar part of the quaternion is $\cos(\theta/2)$ where θ is the angle of rotation. See [41] for other uses of quaternions.

A.2. Protein helices

The protein backbone is formed by a chain of covalently bonded atoms N–C_α–C–N–C_α–C$\cdots$ repeating in units of three atoms. The atoms N are nitrogens and C are (carbonyl) carbons. The atoms C_α are called alpha carbons to which the side chains of the protein are attached. Think of this long chain of atoms as a discrete curve which can be analyzed using the Frenet frames discussed in Section 2. Since the bonds are close to uniform along the backbone, the curvature angles, in this situation called bond angles, are the same at each atom of a given type, C, N or C_α. These angles (angles α and β in Fig. 6) are determined by crystallographic studies and are approximately 60° at N and C. The bonding at the C_α atoms follows tetrahedral geometry so $\cos\gamma = \frac{1}{3}$ and γ is about 70.5°. The bond lengths also approximately depend only on the type of atoms bonded, but that will not concern us here.

Successive atoms C_α–C–N–C_α lie in a plane called the peptide plane and the torsion angle about the C–N bond is assumed to be 180° (π radians). The only degrees of freedom left in the curve are the torsion angles about the N–C_α and C_α–C bonds. The torsion angle about N–C_α is denoted ϕ and the torsion angle about C_α–C is denoted ψ. Often protein databases analyze a structure by listing ϕ and ψ torsion angles along the backbone. We refer to this as a backbone structure.

Regular alpha helical structures have constant ϕ and ψ angles torsion angles. In this paper, as an example, regular alpha helix segments with torsion angles $\phi = -65°$ and $\psi = -40°$ are used. (This is typical for transmembrane proteins, see [42].) Level curves of functions of ϕ and ψ defining properties of protein helices can be graphed on a square $-180° \leqslant \phi \leqslant 180°$, $-180° \leqslant \psi \leqslant 180°$ called a *Ramachandran plane* and such a graph is called a *Ramachandran plot.*

A.3. Helix parameters

A regular helix in a protein secondary structure is given by repetition of a euclidean motion given by a rotation and a translation of the backbone. We consider only the rotational part and the relation between the Frenet frames. We consider the frame F_1 at atom N and F_4 at the subsequent N. If ϕ, ψ are torsion angles at the C_α in between, from Section 2

$$F_4 = F_1R_x(\phi)R_z(\gamma)R_x(\psi)R_z(\alpha)R_x(\pi)R_z(\beta), \tag{22}$$

where $\gamma = \arccos\frac{1}{3}$ is the bond angle at the alpha carbon, and α and β are the bond angles at the C and N atoms respectively. The angles α and β generally differ by less that 3 degrees, so we will assume that $\alpha = \beta$ and (22) becomes

$$F_4 = F_1R_x(\phi)R_z(\gamma)R_x(\psi)R_x(\pi). \tag{23}$$

The product of the four rotations on the right is given by the quaternion

$$e^{I\frac{\phi}{2}}e^{K\frac{\gamma}{2}}e^{I\frac{\psi}{2}}I = \cos\frac{\gamma}{2}Ie^{Is} + \sin\frac{\gamma}{2}e^{tI}J, \tag{24}$$

where

$$s = \frac{\phi+\psi}{2} \quad t = \frac{\phi-\psi}{2}. \tag{25}$$

The unit axis is given by the normalized vector part of the quaternion (24),

$$\mathbf{u} = \frac{1}{\sqrt{1-a^2}}\left(\cos\frac{\gamma}{2}\cos sI + \sin\frac{\gamma}{2}e^{tI}J\right) \tag{26}$$

where

$$a = -\cos\frac{\gamma}{2}\sin s \tag{27}$$

is the scalar part of (24).

If θ is the angle of rotation, $\cos(\theta/2)$ is given by the scalar part of (24),

$$\cos\frac{\theta}{2} = -\cos\frac{\gamma}{2}\sin s. \tag{28}$$

For frames F_j at atoms N on the regular protein helix, where

$$F_{j+3} = F_jR(\mathbf{u},\theta) \text{ where } R(\mathbf{u},\theta) = R_x(\phi)R_z(\gamma)R_x(\psi)R_x(\pi). \tag{29}$$

Eq. (28) can be used to get a simple approximate formula for the rotation angle of a regular helix with torsion angles ϕ and ψ. Squaring both sides of (28) using $\cos\gamma = \frac{1}{3}$ get

$$3\cos\theta = 1 - 4\cos^2\frac{\phi+\psi}{2}, \tag{30}$$

a known formula [43] for the rotation angle θ of a protein helix. For an alpha helix with $\phi = -65°$ and $\psi = -40°$, (30) gives $\theta = 100°$ approximately, or 3.6 residues (C_α atoms) per turn of the helix.

A.4. Symmetry of κ

Two symmetries appear in the Fig. 3 which are not immediately apparent from the geometry of the situation. They are seen in the expression (15), but they can also be deduced from (14) using properties of rotations:

(i) $(\phi,\psi) \leftrightarrow (-\psi,-\phi)$.
This symmetry follows from (14) by taking the transpose to get

$$\cos\kappa = M_3^*R_x(\pi)R_x(-\psi - t_0)R_z(-\gamma)R_x(-\phi + t_0)M_3.$$

Since two R_x rotations commute and $R_x(\pi)R_z(-\gamma) = R_z(\gamma)R_x(\pi)$, get

$$\cos\kappa = M_3^*R_x(-\psi - t_0)R_z(\gamma)R_x(-\phi + t_0)R_x(\pi)M_3. \tag{31}$$

Now comparing with (14), the symmetry follows.

(ii) $(\phi - t_0, \psi + t_0) \leftrightarrow (\psi + t_0, \phi - t_0)$. To see this symmetry, first note that since the third coordinate of M_3 is 0, $R_z(\pi)M_3 = -M_3$. Inserting $-R_z(\pi)M_3$ in place of M_3 in (31) get

$$\cos\kappa = M_3^*R_z(\pi)R_x(-\psi - t_0)R_z(\gamma)R_x(-\phi + t_0)R_x(\pi)R_z(\pi)M_3. \tag{32}$$

Since the two R_z rotations commute and $R_x(\varphi)R_z(\pi) = R_z(\pi)R_x(-\varphi)$ for any φ, it follows that

$$\cos\kappa = M_3^* R_x(\psi + t_0)R_z(\gamma)R_x(\phi - t_0)R_x(\pi)M_3.$$

Now comparing with (14), the symmetry follows.

A.5. Methods

All calculations were performed on personal computers using Maple 11 from Waterloo Maple, Inc. Kinemage files were used to draw the helix model for Fig. 2 and viewed with KiNG [44].

References

[1] J. Hu, T. Asbury, S. Achuthan, C. Li, R. Bertram, J.R. Quine, R. Fu, T.A. Cross, Backbone structure of the amantadine-blocked transmembrane domain M2 proton channel from influenza A virus, Biophys. J. 92 (2007) 4335–4343.

[2] M. Yi, T.A. Cross, H.X. Zhou, Conformational heterogeneity of the M2 proton channel and a structural model for channel activation, Proc. Natl. Acad. Sci. USA 106 (2009) 13311–13316.

[3] A.A. Nevzorov, S.J. Opella, A "magic sandwich" pulse sequence with reduced offset dependence for high-resolution separated local field spectroscopy, J. Magn. Reson. 164 (2003) 182–186.

[4] K. Yamamoto, S.V. Dvinskikh, A. Ramamoorthy, Measurement of heteronuclear dipolar couplings using a rotating frame solid-state NMR experiment, Chem. Phys. Lett. 419 (2006) 533–536.

[5] C.H. Wu, A. Ramamoorthy, S.J. Opella, High resolution heteronuclear dipolar solid-state NMR spectroscopy, J. Magn. Reson. A 109 (1994) 270–272.

[6] T.A. Cross, J.R. Quine, Protein structure in anisotropic environments: development of orientational constraints, Concept NMR 12 (2000) 55–70.

[7] J.R. Quine, T.A. Cross, Protein structure in anisotropic environments: unique structural fold from orientational constraints, Concept NMR 12 (2000) 71–82.

[8] F.M. Marassi, S.J. Opella, A solid-state NMR index of helical membrane protein structure and topology, J. Magn. Reson. 144 (2000) 150–155.

[9] J. Wang, J. Denny, C. Tian, S. Kim, Y. Mo, F. Kovacs, Z. Song, K. Nishimura, Z. Gan, R. Fu, J.R. Quine, T.A. Cross, Imaging membrane protein helical wheels, J. Magn. Reson. 144 (2000) 162–167.

[10] R.R. Ketchem, W. Hu, T.A. Cross, High-resolution conformation of gramicidin A in a lipid bilayer by solid-state NMR, Science 261 (1993) 1457–1460.

[11] K. Nishimura, S. Kim, L. Zhang, T.A. Cross, The closed state of a H+ channel helical bundle: combining precise orientational and distance restraints from solid state NMR, Biochemistry 41 (2002) 13170–13177.

[12] M. Sharma, M. Yi, H. Dong, H. Qin, E. Peterson, D.D. Busath, H.X. Zhou, T.A. Cross, Insight into the mechanism of the Influenza A proton channel from a structure in a lipid bilayer, Science 330 (2010) 509–512.

[13] N.J. Traaseth, R. Verardi, K.D. Torgersen, C.B. Karim, D.D. Thomas, G. Veglia, Spectroscopic validation of the pentameric structure of phospholamban, Proc. Natl. Acad. Sci. USA 104 (2007) 14676–14681.

[14] N.J. Traaseth, L. Shi, R. Verardi, D.G. Mullen, G. Barany, G. Veglia, Structure and topology of monomeric phospholamban in lipid membranes determined by a hybrid solution and solid-state NMR approach, Proc. Natl. Acad. Sci. USA 106 (2009) 10165–10170.

[15] A.A. De Angelis, S.C. Howell, A.A. Nevzorov, S.J. Opella, Structure determination of a membrane protein with two trans-membrane helices in aligned phospholipid bicelles by solid-state NMR spectroscopy, J. Am. Chem. Soc. 128 (2006) 12256–12267.

[16] F.M. Marassi, S.J. Opella, Simultaneous assignment and structure determination of a membrane protein from NMR orientational restraints, Protein Sci. 12 (2003) 403–411.

[17] S.J. Opella, F.M. Marassi, J.J. Gesell, A.P. Valente, Y. Kim, M. Oblatt-Montal, M. Montal, Structures of the M2 channel-lining segments from nicotinic acetylcholine and NMDA receptors by NMR spectroscopy, Nat. Struct. Biol. 6 (1999) 374–379.

[18] S.H. Park, A.A. De Angelis, A.A. Nevzorov, C.H. Wu, S.J. Opella, Three-dimensional structure of the transmembrane domain of Vpu from HIV-1 in aligned phospholipid bicelles, Biophys. J. 91 (2006) 3032–3042.

[19] F.M. Marassi, S.J. Opella, A solid-state NMR index of helical membrane protein structure and topology, J. Magn. Reson. 144 (2000) 994–1003.

[20] R. Soong, P.E.S. Smith, J. Xu, K. Yamamoto, S.C. Im, L. Waskell, A. Ramamoorthy, Proton evolved local-field solid-state NMR studies of cytochrome b5 embedded in bicelles, revealing both structural and dynamical information, J. Am. Chem. Soc. 132 (2010) 5779–5788.

[21] H. Eyring, The resultant electric moment of complex molecules, Phys. Rev. 39 (1932) 746–748.

[22] B.W. Koenig, G. Kontaxis, D.C. Mitchell, J.M. Louis, B.J. Litman, A. Bax, Structure and orientation of a G Protein fragment in the receptor bound state from residual dipolar couplings, J. Mol. Biol. 322 (2002) 441–461.

[23] V. Tugarinov, L.E. Kay, Quantitative NMR studies of high molecular weight proteins: application to domain orientation and ligand binding in the 723 residue enzyme malate synthase G, J. Mol. Biol. 327 (2003) 1121–1133.

[24] W.D. Van Horn, H.J. Kim, C.D. Ellis, A. Hadziselimovic, E.S. Sulistijo, M.D. Karra, C.L. Tian, F.D. Sonnichsen, C.R. Sanders, Solution nuclear magnetic resonance structure of membrane-integral diacylglycerol kinase, Science 324 (2009) 1726–1729.

[25] A. Mascioni, G. Veglia, Theoretical analysis of residual dipolar coupling patterns in regular secondary structures of proteins, J. Am. Chem. Soc. 125 (2003) 12520–12526.

[26] C.M. Franzin, P. Teriete, F.M. Marassi, Membrane orientation of the Na, K-ATPase regulatory membrane protein CHIF determined by solid state NMR, Magn. Reson. Chem. 45 (2007) S192–S197.

[27] B.A. Buck-Koehntop, A. Mascioni, J.J. Buffy, G. Veglia, Structure, dynamics and membrane topology of Stannin: a mediator of neuronal cell apoptosis induced by trimethyltin chloride, J. Mol. Biol. 354 (2005) 652–665.

[28] D.H. Jones, S.J. Opella, Weak alignment of membrane proteins in stressed acrylamide gels, J. Magn. Reson. 171 (2004) 258–269.

[29] L. Shi, N.J. Traaseth, R. Verardi, A. Cembran, J.L. Gao, G. Veglia, A refinement protocol to determine structure, topology, and depth of insertion of membrane proteins using hybrid solution and solid state NMR restraints, J. Biomol. NMR 44 (2009) 195–205.

[30] T. Shimanouchi, S. Mizushima, On the helical configuration of a polymer chain, J. Chem. Phys. 23 (1955) 707–711.

[31] Nobuhiro Go, Harold Scheraga, Ring closure in chain molecules, Macromolecules (1955) 273–281.

[32] Jeffrey K. Denny, Junfeng Wang, T.A. Cross, J.R. Quine, PISEMA powder patterns and PISA wheels, J. Magn. Reson. 152 (2001) 217226.

[33] C. Ramakrishnan, G.N. Ramachandran, Stereochemical criteria for polypeptide and protein chain conformations. II. Allowed conformations for a pair of peptide units, Biophys. J. 5 (1965) 909–933.

[34] K. Gunasekaran, C. Ramakrishnan, P. Balaram, Disallowed conformations of amino acid residues in protein structures, J. Mol. Biol. 264 (1996) 191–198.

[35] S. Hovmöller, T. Zhou, T. Ohlson, Conformations of amino acids in proteins, Acta. Cryst. D D58 (2002) 768–776.

[36] D.B. Dahl, Z. Bohannan, Q. Mo, M. Vannucci, J. Tsai, Assessing side chain perturbations of the protein backbone: a knowledge based classification of residue Ramachandran space, J. Mol. Biol. 378 (2008) 749–758.

[37] M.F. Mesleh, G. Veglia, T.M. DeSilva, F.M. Marassi, S.J. Opella, Dipolar waves as NMR maps of protein structure, J. Am. Chem. Soc. 124 (2002) 4206–4207.

[38] R.C. Page, S. Lee, J.D. Moore, S.J. Opella, T.A. Cross, Backbone structure of a small helical integral membrane prote: a unique structural characterization, Protein Sci. 18 (2009) 134–146.

[39] F.A. Kovacs, J.K. Denny, Z. Song, J.R. Quine, T.A. Cross, Helix tilt of the M2 transmembrane peptide from influenza A virus: an intrinsic property, J. Mol. Biol. 295 (2000) 117–125.

[40] M.F. Mesleh, S. Lee, G. Veglia, D.S. Thiriot, F.M. Marassi, S.J. Opella, Dipolar waves map the structure and topology of helices in membrane proteins, J. Am. Chem. Soc. 125 (2003) 8929–8935.

[41] J.R. Quine, Helix parameters and protein structure using quaternions, J. Mol. Struct. (Theochem) 460 (1999) 53–66.

[42] Richard C. Page, Sanguk Kim, Timothy A. Cross, Transmembrane helix uniformity examined by spectral mapping of torsion angles, Structure 16 (2008) 787–797.

[43] R.E. Dickerson, I. Geis, Structure and Action of Proteins, Harper, New York, 1969.

[44] V.B. Chen, I. Davis, D.C. Richardson, KiNG (Kinemage next generation): a versatile interactive molecular and scientific visualization program, Protein Sci. 18 (2009) 2403–2409.